Quantum tunneling in magnetic tunneling junctions

Evgeni S. Cruz de Gracia
Facultad de Ingeniería Eléctrica
Universidad Tecnológica de Panamá
evgeni.cruz@utp.ac.pa

Lucio Strazzabosco Dorneles, Luiz Fernando Schelp
Departamento de Física
Universidad Federal de Santa María, Brasil
lsdorneles@gmail.com, fschelp@gmail.com

Sérgio Ribeiro Teixiera, Mario Norberto Baibich
Instituto de Física
Universidad Federal de Río Grande del Sur, Brasil
srgrbrtxr@gmail.com, mbaibich@gmail.com

Abstract - *This paper reports on the study of ferromagnetic tunneling junctions produced by magnetron sputtering technique and deposited under oxidation conditions that lead to low potential barrier height, low asymmetrical barrier and quantum tunneling as the charge transport mechanism. The exponential growth of the effective area-resistance product with the effective barrier thickness, and the concentration of the tunnel current in small areas of the junctions, were identified by fitting room temperature I-V curves, for each individual sample, with either Simmons' [J. Appl. Phys. 34, 1793 (1963); 35, 2655 (1964); 34, 2581 (1963)] or Chow's [J. Appl. Phys. 36, 559 (1965)] model. This result suggests the presence of effective tunneling areas or hot spots, leading to a non-uniform current distribution and showing quantum tunneling as the charge transport mechanism. This mechanism, is also, verified through I-T curves.*

Keywords - *Electronic transport, junction, magnetization, tunneling.*

Resumen - *Este artículo reporta sobre el estudio de la juntura túnel ferromagnética producida por la técnica de erosión iónica y depositada bajo condiciones de oxidación que llevan a baja altura de la barrera de potencial, baja asimetría de la barrera y el tunelamiento cuántico como mecanismo de transporte electrónico. El crecimiento exponencial del producto de la resistencia por el área efectiva detunelamiento en función del espesor efectivo de la barrera y la concentración de la corriente detunelamiento enpequeñas áreas de la juntura túnel fueronidentificados a través delajuste de las curvas I-V medidas a temperatura ambiente, para cada muestra individual, usando ya sea el modelo de Simmons [J. Appl. Phys. 34, 1793 (1963); 35, 2655 (1964); 34, 2581 (1963)] como el de Chow [J. Appl. Phys. 36, 559 (1965)]. Este resultado sugiere la presencia de áreas efectivas para tunelamiento o focos caliente que nos lleva a una distribución no uniforme de la corriente y muestra el tunelamiento cuántico como mecanismo de transporte electrónico. Este mecanismo, también es verificado a través de las curvas I-T.*

Palabras Claves - *Juntura, magnetización, Transporte electrónico, tunelamiento.*

1. INTRODUCTION

The field of research in spin engineered materials is very active on account of its richness in physical phenomena and technological applications. Among the spin device arrangements, the magnetic tunneling junction (MTJ) is the simplest structure which consist basically of two magnetic layers (electrodes) separated by a thin insulating layer (barrier). Electrodes can be deposited from partially spin polarized materials (3d ferromagnetic metals such as Fe, Co, Ni or its alloys) or completely spin polarized materials such as half metals (Bi and La1-xSrxMnO3). The insulating layer can be obtained by plasma oxidation of metallic Al. More recently, MgO has been widely reported. MTJs are incorporated in non-volatile magnetic random access memories (MRAM), racetrack memories, sensor heads and biomedicine applications.

The study of transport phenomena in MTJs, on account of the many possible mechanisms, entails a systematic analysis of experimental data. The most exploited phenomenon in MTJs has been the tunneling conductivity behavior with applied magnetic field. This phenomenon is called tunnel magnetoresistance (TMR) and is very attractive for spin engineered materials. In spite of the tremendous number of works in this particular field, the TMR bias dependence and the tunneling resistance behavior with barrier thickness still remains not well understood.

At the beginning, experiments on quantum tunneling were used to reveal the electronic structure of superconductor materials. Later, by applying a strong magnetic field these experiments were used to study the density of states (DOS) of these materi-

als through measurements of conductivity as a function of the applied bias.

The exponential growth of resistance with increasing barrier thickness is an important criterion to verify quantum tunneling in the junction's electronic transport. This comes among many other criteria, such as tunnel current behavior as a function of temperature (I-T), breakdown voltages and I-V curve shapes [1]. Although the exponential growth of resistance is a necessary condition for quantum tunneling, it is not a sufficient one [2]. It is, also, the most fundamental and difficult to be determined.

This difficulty may be ascribed to the imprecise determination of the actual insulating barrier thickness involved in the tunneling process, which defines the actual current density. Electronic transport measurements, I-V curves in our case, are sensitive to small fractions of the barrier thickness and tunneling area due to the thickness fluctuations occurring during the growth of the films.

Transmission electron microscopy (TEM) and grazing incidence x-ray reflectivity (GIXR) are powerful tools for thin films thickness determination, but the visualized area for TEM may sometimes not be representative of the effective junction area as a whole [3]-[4]. On the other hand, GIXR determines an average thickness over relatively large areas. As a matter of fact, thickness values determined from TEM and GIXR are usually higher than those deduced from electronic transport [5]. Buchanan et al. [6], using GIXR, showed that the insulating barrier thickness is, in all cases, much larger than the thickness of the initial Al metallic layer before oxygen incorporation and twice the value determined from the I-V curves fitting. As a matter of fact, results for insulating thickness extracted from GIXR, TEM and I-V curves should converge only in small and strictly perfect junctions. In this context, fitting of the I-V from model curves is helpful because the current will intrinsically probe the relevant part of the junction.

These differences in thickness suggest that the tunneling current is concentrated in small regions, or hot spots, of the total junction area [7]-[8]. It is therefore reasonable to leave not only the barrier thickness and potential height as free parameters for the fitting procedure of I-V curves, but also the junction area. Dorneles et al. [5] showed a consistent result for the exponential growth of the effective area resistance product (RAeff) as a function of the effective barrier thickness for non-magnetic

tunneling junctions, Al/AlOx/Al, using intrinsic barrier parameters extracted from I-V curves with Simmons's model for symmetric tunnel barrier [9]-[10]. The physical meaning of Aeff for hot spots would be the effective area covered by the thinnest barrier, where the tunnel current is supposed to be concentrated.

In this work we take advantage of the fact that the intrinsic barrier parameters (thickness and potential height) are correlated, and that we cannot precisely control the effective area of hot spots. We leave, therefore, the junction area as a free parameter, with barrier thickness and potential barrier height to fit room temperature I-V curves with either Simmons' [9]-[11] or Chow's [12] models for MTJs. An exponential growth of the normalized resistance (R.Aeff) with the effective barrier thickness is found for MTJs with low potential barrier height and low asymmetrical barrier showing quantum tunneling as the charge transport mechanism. This mechanism, is also, verified through I-T curves.

2. EXPERIMENTAL

Samples were deposited from pure (99.99%) bulk targets by magnetron sputtering with typical base pressure of 10-7 mbar (or lower), using masks to define 200 μm electrodes in the crossed stripe geometry with a 4 × 10-4cm2 junction area. Material stack was deposited on glass substrate and consist of: Ta(98)/Py(474)/Al(20)Ox(Y)/Co(420)/ /Cu(100), where Y=30s, 45s and 60s stand for the oxidation time process (Tox), and all the nominal thickness are in Å. The insulating barrier was deposited by glow discharge assisted oxidation of a thin Al (20Å) film in a 100 mbar O2 atmosphere.

I-V curves were measured using the four point probe method in a DC low noise system. This system allows noise rejection and has input impedance greater than 10 GΩ. A standard resistor in series with the sample is used to detect the sample's current flow. A homemade differential instrumentation amplifier then amplifies the measured voltage.

2.1 Fitting Procedures

The fitting procedure for the I-V curves was done using Simmons' [9]-[11] and Chow's models [12]. Both models evaluate the tunnel current density using the Wentzel-Kramers-Brillouin (WKB) approximation for tunneling probability, differing on the approach to solve the integrals. While the first approximates the arbitrary potential barrier φ(x, V) to a mean barrier height [ ], the second approximates any arbitrary potential barrier

by an equivalent rectangular barrier whose height is determined by the root mean square value of the arbitrary potential barrier. This leads to a dependence of bias polarity for asymmetrical tunnel barriers. In order to compare the tunnel current density with the experimental data, an explicit potential barrier shape must be assumed. Also, while fitting the experimental curves with the models, the junction area was left as an additional free parameter to contemplate the presence of hot spots [13]-[15].

For similar electrodes and nonzero temperatures both models assume a rectangular potential barrier, so the tunnel current density is given in practical units for Simmons' and Chow's models by:

$$J(V,T) = \left(\frac{6.2 \times 10^{10}}{t^2}\right)\left(\left(\varphi_0 - \frac{V}{2}\right)\exp\left[-1.025\ t\left(\varphi_0 - \frac{V}{2}\right)^{\frac{1}{2}}\right] - \left(\varphi_0 + \frac{V}{2}\right)\text{X}\right.$$

$$\left.\exp\left[-1.025\ t\left(\varphi_0 + \frac{V}{2}\right)^{\frac{1}{2}}\right]\right)\left(1 + \left[\frac{3 \times 10^{-9} t^2 T^2}{\left(\varphi_0 - \frac{V}{2}\right)}\right]\right), \qquad (1)$$

and

$$J(V,T) = \left(\frac{9.2484 \times 10^{10}}{t^2}\right)\left(\varphi_r \exp\left[-1.025\ t(\varphi_r)^{\frac{1}{2}}\right] - \left(\varphi_r + V\right)\text{X}\right.$$

$$\left.\exp\left[-1.025\ t\left(\varphi_r + V\right)^{\frac{1}{2}}\right]\right)\left(1 + \left[\frac{3 \times 10^{-9} t^2 T^2}{\varphi_r}\right]\right), \qquad (2)$$

respectively. In the expressions, T stands for temperature and the free parameters are the rectangular potential barrier $\varphi_0(V)$, the insulating barrier thickness t (Å), and the junction area A (cm2) which is related to the measured tunnel current (I) through $J(V,T) = I/A$.

Also, φ_r is the equivalent rectangular barrier height given by:

$$\varphi_r = \frac{4}{9}\left(\left[\varphi_0^{\frac{3}{2}} - \left(\varphi_0 - V\right)^{\frac{3}{2}}\right] \times V^{-1}\right)^2, \qquad (3)$$

For dissimilar electrodes and nonzero temperatures, both models assume a trapezoidal potential barrier. In this work we assume the tunnel current density in the reverse direction, that is, electrode 2 (Py) is positively biased with respect to electrode 1

(Co). In practical units for Simmons' and Chow's models the tunnel current is given by:

$$J_{1\to2}(V,T) = \left(\left(\varphi_1 + \varphi_2 - V\right)\exp\left[-0.7244\ t\left(\varphi_1 + \varphi_2 - V\right)^{\frac{1}{2}}\right] - \right.$$

$$\left.\left(\varphi_1 + \varphi_2 + V\right)\exp\left[-0.7244\ t\left(\varphi_1 + \varphi_2 + V\right)^{\frac{1}{2}}\right]\right)\left(\frac{3.6537 \times 10^{10}}{t^2}\right)\text{X}$$

$$\left(1 + \left[\frac{6 \times 10^{-9} t^2 T^2}{\left(\varphi_1 + \varphi_2 - V\right)}\right]\right), \qquad (4)$$

and

$$J_{1\to2}(V,T) = \left(\frac{9.2484 \times 10^7}{t^2}\right)\left(\varphi_{r_{12}} \exp\left[-1.025\ t\left(\varphi_{r_{12}}\right)^{\frac{1}{2}}\right] - \right.$$

$$\left.\left(\varphi_{r_{12}} + V\right)\exp\left[-1.025\ t\left(\varphi_{r_{12}} + V\right)^{\frac{1}{2}}\right]\right)\text{X}$$

$$\left(1 + \left[\frac{3 \times 10^{-9} t^2 T^2}{\varphi_{r_{12}}}\right]\right), \qquad (5)$$

respectively. The parameter φ_{r12} is the effective barrier height and is given by:

$$\varphi_{r_{12}} = \frac{4}{9}\left(\left[\varphi_1^{\frac{3}{2}} - \left(\varphi_2 - V\right)^{\frac{3}{2}}\right] \times \left[\varphi_1 - \varphi_2 + V\right]^{-1}\right)^2, \qquad (6)$$

and φ_1, and φ_2 (free parameters) are the potential barrier heights at the interfaces between the insulating barrier and electrodes 1 and 2, respectively.

It should be noted that all equations are in the intermediate voltage range, that is, $0 \le V \le \varphi_0$ for similar electrodes and $0 \le V \le \varphi_2$ for dissimilar ones. Also, the potential barrier height has a bias dependence, and when $\varphi_1 = \varphi_2$, all equations reduce to similar electrode equations.

3. RESULTS AND DISCUSSION

Figure 1 shows *I-V* curves for a Py/Al(20Å)Ox(30s)/Co sample with a linear shape for $V \to 0$ and a non ohmic behavior above 150 mV. The moderate increases of the low voltage electrical resistance when the temperature decreases, together with the I-V curve shape indicate quantum tunneling as the charge transport mechanism [16]. For $V \to 0$

the first exponential factor on the right hand side of equation 5, corresponding to the first quadrant of figure 1, has a small contribution, leaving only the linear contribution for the I-V characteristic.
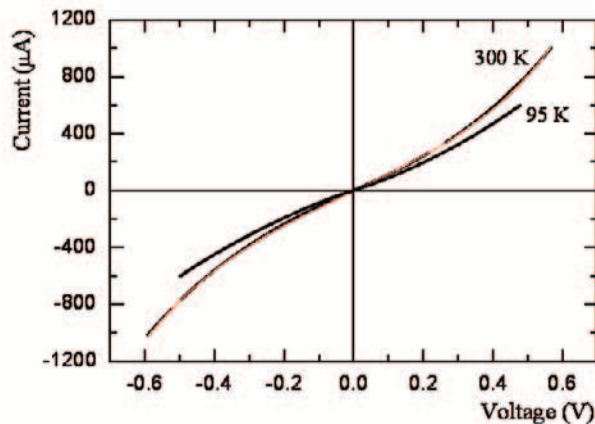

Figure 1. Experimental room temperature *I-V* curve fitted using Chow's model for asymmetrical tunnel barrier showing experimental curve (points) and simulated one (line). The ferromagnetic electrodes are in the parallel state of magnetization. Some experimental points have been left out intentionally to show the quality of the fit. I-V curve for 95 K shows a resistance increase with a decrease in temperature [17].

For $V \leq \varphi 2$ the exponential factor has a larger contribution than the linear one, approximately one order of magnitude higher than the normalized value for $V \rightarrow 0$, leading to a nonlinear behavior, as can also be seen on figure1. The low-voltage ohmic and the non ohmic behavior of the I-V curves appear at both low and room temperatures, with or without an applied magnetic field [17].

Physically this means that the bias shifts the Fermi level of one electrode with respect to the other, and the effective barrier height decreases, so more electrons can tunnel because there are more empty states available on the second electrode, increasing the transmission coefficient. As a consequence, the barrier resistance decreases. Figure 2 shows a schematic energy diagram illustrating this idea for both regions.

Also, figure 1 shows the room temperature fit using Chow's model for asymmetric tunnel barrier, where the experimental curve can hardly be differentiated from the fitted one. This I-V curve behavior can be reasonably well described also by Simmons' model, on account of the small potential asymmetry. The values obtained by the fitting procedures, for a group of samples, are shown in Table 1. Several aspects of these parameters merit to be addressed.
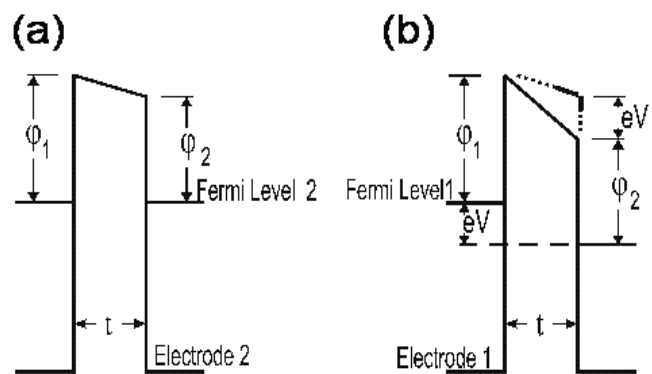

Figure 2.(a) Schematic energy diagram for low voltage region $V \rightarrow 0$ and (b) for intermediate voltage region $0 \leq V \leq \varphi 2$. The electrode 2 is positively biased with respect to the electrode 1 [17].

First, under our experimental conditions, neither the barrier height nor its thickness is strongly affected by the oxidation time. We interpret this as a signature of the presence of hot spots. The mean oxide thickness, measured with low angle RX diffraction, increases almost linearly with oxidation time, but this will not be relevant for the tunneling when the current concentrates in small portions of the sample. As can be seen on Table 1, the effective tunneling areas extracted from the fittings represent less than 1% of the junction's geometrical area, a percentage that is near those found by scanning tunneling microscopy (STM). The extracted values for barrier thickness are around 10 Å, smaller than the values usually reported for similar junctions but close to those extracted by fitting of I-V curves measured using STM tips [18].

It should be mentioned here that considering the effective tunneling area in the fitting procedure limits the errors induced by interface roughness, as has been proved by modeling and simulations [14]. If the values obtained for all the samples are put together they compose a consistent picture, showing the expected exponential growth of the normalized resistance (RA_{eff}) versus effective barrier thickness (t_{AlOx}) as depicted in figure 3 for data taken from Table 1 corresponding to Chow's model for symmetric tunnel barrier[17].

Figure 3 suggest that quantum tunneling is indeed the charge transport mechanism. A slight increase of 3 Å in barrier effective thickness is in agreement with two orders of magnitude change for RAeff .This is a robust result and leaves no doubt about quantum tunneling for MTJs, but also suggest the

Table1. Barrier's intrinsic parameters extracted from fittings of I-V curves using Simmons' [22]-[24] and Chow's models [25]. Barrier effective thickness (t$_{AlOx}$), barrier potential height (φ), effective tunneling area (A$_{eff}$) and oxidation time (T$_{ox}$). I-V curves measured at 300 K and ferromagnetic electrodes in the antiparallel state of magnetization [17].

| | Symmetric Barrier | | | | Asymmetric Barrier | |
| | Simmons | | Chow | | Chow | |
T$_{ox}$(s)	φ_o (eV)	t_{AlOx} (Å)	φ_o (eV)	A_{eff}(cm^2)	φ_1 (eV)	φ_2 (eV)
30	0.726 ± 0.014	8.98 ± 0.08	0.778 ± 0.017	(2.9 ± 0.4)E-9	1.221 ± 0.018	0.985 ± 0.014
30	0.743 ± 0.004	9.39 ± 0.08	0.827 ± 0.006	(1.9 ± 0.3)E-9	1.239 ± 0.015	1.032 ± 0.019
30	0.807 ± 0.023	9.96 ± 0.18	0.914 ± 0.035	(1.2 ± 0.4)E-8	1.231 ± 0.025	0.990 ± 0.011
45	0.819 ± 0.021	10.14 ± 0.20	0.926 ± 0.032	(2.1 ± 0.3)E-8	1.236 ± 0.024	1.002 ± 0.023
45	0.793 ± 0.006	10.53 ± 0.07	0.945 ± 0.013	(1.1 ± 0.1)E-8	1.251 ± 0.013	1.018 ± 0.022
60	0.836 ± 0.024	10.98 ± 0.11	0.990 ± 0.017	(3.9 ± 0.4)E-8	1.269 ± 0.011	1.034 ± 0.017
60	0.845 ± 9E-4	11.71 ± 0.20	1.039 ± 0.007	(3.5 ± 0.7)E-8	1.308 ± 0.029	1.075 ± 0.025

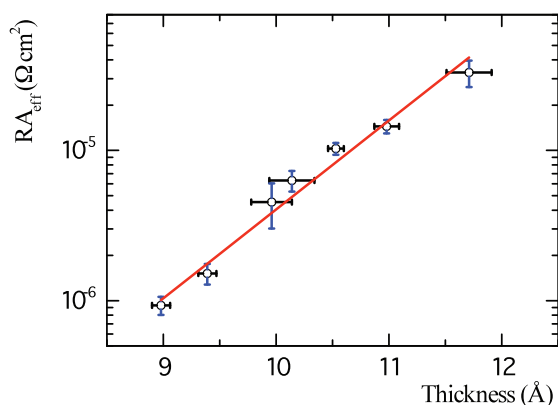Figure 3.Room temperature effective area resistance product (R.A$_{eff}$) as a function of the tunneling effective barrier thickness (t$_{AlOx}$). Low voltage electrical resistance determined in the linear range of I-V curves between –40mV and +40mV. The continuous line has been calculated according to the expression $P \exp\left[\frac{2\,t_{AlOx}}{\hbar}\sqrt{2\,m\,\varphi_o}\right]$ where P = 7.4x10-12 Ω cm2 and φo = 1.4 eV. For this expression the potential barrier height (φo) is an independent function of the t$_{AlOx}$, and the effective mass of the tunneling electron within the barrier is neglected [17].

presence of hot spots. In this particularly case Aeff scales from 10^{-8} to 10^{-9}cm^2, as can be seen on table 1. If compared with the physical junction area of about 4 x 10^{-4}cm^2, we conclude that there must be an effective tunneling area, indicating the presence of hot spots. During the bottom electrode thin film deposition there will always be thickness fluctuations. These fluctuations define regions where both electrodes will remain closer (hot spots).

The last two columns on the right hand side of Table 1 show the potential barrier heights φ1 and φ2 for asymmetric tunnel barrier, as shown in figure 2, where φ1 and φ2 are the potential barrier height at the first and second metal/insulator/metal interfaces, respectively. The asymmetry (Δφ) is roughly 0.2 eV, meaning that the MTJs have an almost rectangular potential barrier (φ1≈ φ2). The low asymmetry is usually correlated to properly oxidized tunnel barriers with a strong glow discharge [19] but also reflects the similar work function values for both electrodes. On the other hand, this result also justifies why simulations for symmetric tunnel barrier show good agreement with experimental I-V curves for both models.

As can be seen on Table 1, for Simmons' and Chow's models simulations we have values of φ ≤ 1.0 eV, meaning that we have deposited samples with low potential barrier height values, if compared to values reported in the literature for the same system (φ ≥ 1.9 eV) [20]-[21]. We can argue about the physical reasons for this low potential barrier. It could be due to deviation from Al2O3 stoichiometry in the regions relevant for the tunneling transport. Up to now, we do not have an experimental method to follow locally the composition of the oxide. Another possibility is that a build-up process of the tunnel barrier is present indicating that for very thin oxide layers the insulator gap has not yet been com-

pletely established.

Finally, the other accepted criterion to verify quantum tunneling as the charge transport mechanism is presented in figure 4, showing the tunnel current behavior as a function of temperature for a constant applied bias of 300 mV and 40 mV. This result is in accordance with Stratton's model (1962) [22]. This model takes on account thermal energy contribution for the tunnel current and is given by:

$$I(T) = I(0)[1 + C\,T^2 + ...]\,, \qquad (7)$$

whereI(0) represents tunnel current for zero temperature and C is a constant which depends on barrier´s intrinsic parameters (t e φ).

As predicted by Stratton, tunnel current is proportional to T^2 in the whole temperature range for a constant applied bias of 300 mV and 40 mV.
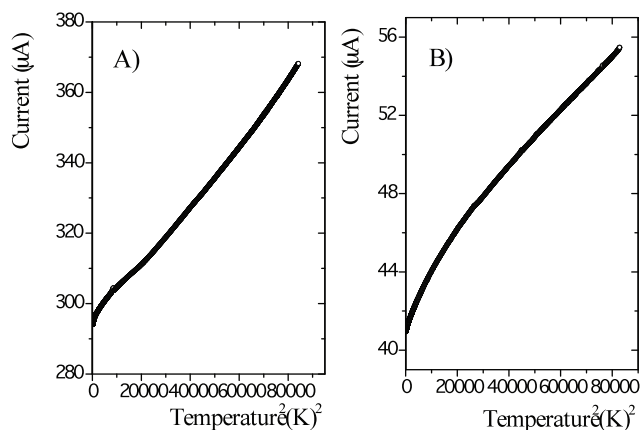

Figure 4. Experimental curves of tunnel current as a function of temperature for a Py/Al(17 Å)Ox(45 s)/Co MTJ. Curve (A) for a constant applied bias of 300 mV and (B) for 40 mV.

4. CONCLUSIONS

Electronic transport measurements, I-V curves, are sensitive to small fractions of the barrier thickness and tunneling area. This is helpful because the current will intrinsically probe the relevant part of the junction. It means that leaving the junction area as free parameter, together with barrier thickness and potential barrier height, lead us to coherent results for fitting I-V curves. Following this idea, an expected exponential growth of the effective area-resistance product with the effective barrier thickness for MTJs with low potential barrier height and low asymmetrical barrier, was found. Therefore we can conclude that tunnel current concentrates in

small areas of the junctions (less than 1% of the junction's geometrical area).

This result composes a consistent picture showing that quantum tunneling is indeed the charge transport mechanism for our MTJs. I-T curves, are also consistent with this picture.

6. REFERENCES

[1] U. Rudiger, R. Calarco, U. May, K. Samm, J. Hauch, H. Kittur, M. Sperlich, and G. Guntherodt, J. Appl. Phys. 89, 7573 (2001).

[2] B.J. Jonsson-Akerman, R. Escudero, C. Leighton, S. Kim, I.K. Schuller, and D.A. Rabson, "Reliability of normal-state current-voltage characteristics as an indicator of tunnel-junction barrier quality," Appl. Phys. Lett. v.77, n.12, pp.1870 Sept. 2000.

[3] S. Yuasa, T. Nagahama, and Y. Suzuki, "Spin polarized resonant tunneling in magnetic tunnel junctions," Science v.297, n.5579, pp.234 237, 2002.

[4] S. Yuasa, T. Sato, E. Tamura, Y. Suzuki, H. Yamamori, K. Ando, and T.Katayama, "Magnetic tunnel junctions with single-crystal electrodes: A crystal anisotropy of tunnel magnetoresistance," Europhys. Lett.v.52, n.3, pp.344-350, 2000.

[5] L.S. Dorneles, D.M. Schaefer, M. Carara, and L.F. Schelp, "The use of Simmons equation to quantify the insulating barrier parameters in Al/AlOx/Al tunnel junctions," Appl. Phys. Lett., v. 82, n. 17, pp. 2832-2834, Apr. 2003.

[6] J.D.R. Buchanan, T.P.A Hase, B.K. Tanner, N.D. Hughes, and R.J. Hicken, "Determination of the thickness of Al2O3 barriers in magnetic tunnel junctions," Appl. Phys. Lett.v.81, n.4, pp.751-753, 2002.

[7] V. da Costa, F. Bardou, C.Béal, Y. Henry, J.P. Bucher, and K.Ounadjela, "Nanometric cartography of tunnel current in metal-oxide

junctions," J. Appl. Phys., v.83, n.11, pp.6703-6705, June 1998..

[8] T. Dimopoulos, V. da Costa, C. Tiusan, K. Ounadjela, and H.A.M. van der Berg, "Local investigation of thin insulating barriers incorporated in magnetic tunnel junctions," J. Appl. Phys., v. 89, n. 11, p. 7371-7373, June 2001.

[9] J.G. Simmons, "Generalized formula for the electric tunnel effect between similar electrodes separated by a thin insulating film," J. Appl. Phys., v.34, n.6, pp. 1793-1803, June 1963.

[10] J.G. Simmons, "Generalized thermal J-V characteristic for the electric tunnel effect," J. Appl. Phys., v.35, n.9, p.2655-2658, Sept. 1964.

[11] J.G. Simmons, "Electric tunnel effect between dissimilar electrodes separated by a thin insulating film," J. Appl. Phys., v.34, n.9, p.2581-2590, Sept. 1963.

[12] C.K. Chow, "Square-mean-root approximation for evaluating asymmetric tunneling characteristics," J. Appl. Phys., v.36, n.2, p.559-563, Aug. 1965.

[13] Philip C. D., Hobbs, Robert B., Laibowitz, and Frank R. Libsch, Appl. Optics v.44, n.32, pp.6813, 2005.

[14] Casey W. Miller, Zhi-Pan Li, JohamAkerman, and Ivan K. Schuller, "Impact of interfacial roughness on tunneling conductance and extracted barrier parameters," Appl. Phys. Lett. v90, n.4pp.043513, Jan. 2007.

[15] V. Da Costa, C. Tiusan, T. Dimopoulos, and K. Ounadjela, "Tunneling phenomena as a probe to investigate atomic scale fluctuations in metal/oxide/metal magnetic tunnel junctions," Phys. Rev. Lett., v. 85, n.4, p. 876-879, July 2000.

[16] T. Miyazaki, and N. Tezuka, "Spin-polarized tunneling magnetoresistive effect in ferromagnet/insulator/ferromagnet junctions,"J. Magn.Magn.Mater.v.151, pp.403, 1995.

[17] E. S. Cruz de Gracia, L. S. Dorneles, L. F. Schelp, S. R. Teixeira and M. N. Baibich, "Low potential barrier height effects in magnetic tunneling junctions," Phys. Rev. B.,

v.76, pp.214426, 2007.

[18] V. Da Costa, Y. Henry, F. Bardou, M. Romeo, and K. Ounadjela, "Experimental evidence and consequences of rare events in quantum tunneling," The European Physical Journal B, v. 13, pp.297-303, Apr. 2000.

[19] J. Nowak, D. Song, E. Murdock, "Dynamic conductance of Ni80Fe20 /Al2O3/ Ni80Fe20 tunnel junctions," J. Appl. Phys., v.87, n.9, p.5203-5205, May 2000.

[20] J. S. Moodera, L. R. Kinder, T. M. Wong, and R. Meservey, "Large magnetoresistance at room temperature in ferromagnetic thin film tunnel junctions," Physical Review Letters, v.74, n.16, p.3273-3276, Apr. 1995.

[21] H. Boeve, E. Girgis, J. Schelten, J. De Boeck, and G. Borghs, "Strongly reduced bias dependence in spin-tunnel junctions obtained by ultra violet light assisted oxidation," Appl. Phys. Lett., v.76, n.8, p.1048-1050, Fev. 2000.

[22] R. Stratton, "Volt current characteristics for tunneling through insulating films," Journal of Physics and Chemistry of Solids, v.23, p.1177-1190, Mar. 1962.